A simulation study on p-doping level of polymer host material in P3HT:PCBM bulk heterojunction solar cells

Hossein Movla† and Mohammad Babazadeh

Azar Aytash Co., Technology Incubator, University of Tabriz, Tabriz, Iran

(Received 1 February 2016; revised manuscript received 26 November 2016; published online 20 February 2017)

In this study, we investigate the influence of doping on the charge transfer and device characteristics parameters in the bulk heterojunction solar cells based on poly(3-hexylthiophene) (P3HT) and a methanofullerene derivative (PCBM). Organic semiconductors are also known to be not pure and they have defects and impurities, some of them are being charged and act as p-type or n-type dopants. Calculations of the solar cell characteristics parameters versus the p-doping level have been done at three different n-dopings (N_d) that consist of 5×10^{17} cm^{-3}, 10^{18} cm^{-3}, and 5×10^{18} cm^{-3}. We perform the analysis of the doping concentration through the drift-diffusion model, and calculate the current and voltage doping dependency. We find that at three different n-dopant levels, optimum p-type doping is about $N_p = 6\times10^{18}$ cm^{-3}. Simulation results have shown that by increasing doping level, V_{oc} monotonically increases by doping. Cell efficiency reaches its maximum at somewhat higher doping as FF has its peak at $N_p = 3\times10^{18}$ cm^{-3}. Moreover, this paper demonstrates that the optimum value for the p-doping is about $N_p = 6\times10^{18}$ cm^{-3} and optimum value for n-dopant is $N_d = 10^{18}$ cm^{-3}, respectively. The simulated results confirm that doping considerably affects the performance of organic solar cells.

Keywords: organic photovoltaics, charge transport, doping, finite difference method

PACS: 88.40.jr, 91.60.Tn, 61.72.-y, 02.70.Bf **DOI:** 10.1088/1674-1056/26/4/048802

1. Introduction

In recent years, there have been interests in research in the field of the organic bulk heterojunctions formed by an interpenetrating blend of optically active polymers and electron accepting molecules.[1–3] The organic semiconductor is the base of the modern electronic and optoelectronic devices such as organic light emitting diodes (OLEDs), organic solar cells (OSC), organic field effect transistors (OFET), and so on.[4,5] Efficient and low cost production, physical flexibility and non-toxic property of organic semiconductors make them a good alternative to common inorganic semiconductors, especially for solar energy applications.[6,7] The currently most efficient class of OSC has an absorber consisting of a blend of donor and acceptor molecules together, which creates a heterojunction throughout the bulk of the device.

Schematic diagrams of the bulk heterojunction solar cells based on poly(3-hexylthiophene) (P3HT) and a methanofullerene derivative (PCBM) is shown in Fig. 1(a) and the detailed transport of generated charge carriers in blend materials is shown in Fig. 1(b).

As it can be seen in Fig. 1(b), holes transport only in donor material and electrons transport through acceptor materials which is completely different from inorganic solar cells in which electrons and holes transport and recombine in the same material. In the OSCs, there are two different pathways in transport of electrons and holes, that leads to different transport mechanisms for charge carrier, and due to the highly disordered properties, device physics of organic semiconductors are very different from inorganic types.[8] It was found that the structures and the properties of organic solar cells (OSCs) highly depend upon both the fabrication methods and materials in use, thus many experiments, models and numerical simulations have been developed to understand the physical behavior and performance of organic devices.[9–11] In addition to experimental studies, numerical device models for the electronic and optical processes allow researchers a good understanding and also efficient optimization of organic optoelectronics devices.[12–15] To model BHJ solar cells, it was proposed to start with the metal–insulator–metal (MIM) scheme, where the active region of the cell, which consists of the bulk heterojunction layer, is considered as one virtual semiconductor with the properties of both the donor and acceptor.[16–21]

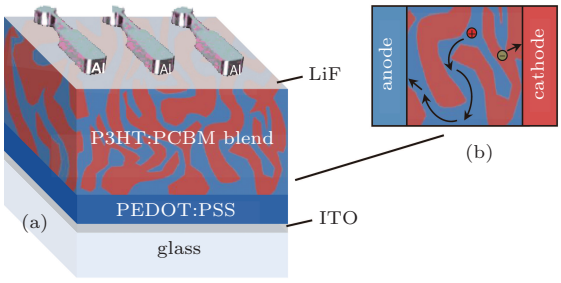


Fig. 1. (color online) (a) Schematic diagrams of the P3HT:PCBM bulk heterojunctions organic solar cell and (b) free charge transport toward the electrodes.

Unlike inorganic semiconductor materials, organic semiconductors are usually prepared in a nominally undoped form.[22] However, controlled and stable doping is a prereq-

†Corresponding author. E-mail: h.movla@azaraytash.com

© 2017 Chinese Physical Society and IOP Publishing Ltd

uisite for the realization and the efficiency of many organic-based devices.[22] Organic semiconductors are also known to be not pure and they have defects and impurities, of which some of them are being charged.[23–25] The charged defects can act as dopants and affect the exciton dissociation and charge transport in the active layer of organic solar cells.[26] The basic principle of p-type or n-type doping in organic semiconductors is similar to that in inorganic materials: one has to add impurities which either transfer an electron to the electron-conducting states (n-type doping) or remove an electron from the hole-conducting states to generate a free hole.[22,27,28] There is a general problem for n-doping in which the matrix materials should be acceptors, however, a sufficient purification of these materials was not reached until now.[22,29]

In most OSCs numerical studies, doping of the active region has been ignored and it has been assumed that organic semiconductors are intrinsic or undoped, however, in a comprehensive and consistent device model, it cannot be ignored.[20,26]

In this paper, we present a numerical simulation to investigate the influence of p-type doping on the performance of OSCs. The main goal of our work is to understand the effects of p-dopant in the active region on the characteristic parameters of solar cell at low mobility. The electrical behavior of OSCs can be predicted by solving a self-consistent drift-diffusion numerical model where, in this study, by solving self-consistent drift-diffusion and Poisson equations via finite element method (FEM) and considering the boundary condition, short circuit current (J_{sc}), open circuit voltage V_{oc}, fill factor (FF), η, and J–V characteristics have been calculated in terms of p-doping concentration. In many of the earlier reports, the basic type of charge carrier recombination was set as the Langevin type or bimolecular, but this type of recombination in some cases failed to exactly determine charge carrier and recombination processes.[17,18,20,30] So, by developing the physics of OSCs in detail, different recombination models have been suggested. In this study, different recombination models such as bimolecular or Langevin recombination, Shockley–Read–Hall (SRH) recombination or trap-assisted and geminate recombination, have been taken into account in numerical simulations.

2. Models and Methods

The device is described by using the metal–insulator–metal picture.[31] This means that the device is thought of to be built up by one semiconductor with the lowest unoccupied molecular orbit (LUMO) of the acceptor and the highest occupied molecular orbit (HOMO) of the donor as valence and conduction band, respectively; see Fig. 1 for the energy levels of both organic materials and metal contacts. Bimolecular or Langevin recombination, R_0, with the recombination constant (β) and the intrinsic charge carrier density (n_i), that is governed by electron (n) and hole (p) density is given by the following equation

$$R_{lang} = \beta(np - n_i^2), \tag{1}$$

which Langevin theory gives a description of β as a function of mobilities of electron and hole, μ_n and μ_p, respectively:

$$\beta = q\frac{(\mu_n + \mu_p)}{\varepsilon\varepsilon_0}. \tag{2}$$

In this equation, $\varepsilon\varepsilon_0$ is the permittivity of the active layer material and q is the elementary charge, μ_n and μ_p are electron and hole mobility, respectively. For the pristine materials, charge carriers both belong to the same material and could move in all directions while the recombination occurs in a point near to the charge carrier having low mobility.[15,32] In our simulation, we assume the mobilities of electrons and holes are the same. The photogeneration of free charge carriers has been explained by the Onsager theory[33] and Braun[34] has made an important refinement to this theory by pointing out that the bound electron–hole pair with binding energy E_B, which acts as a precursor for free charge carriers, has a finite lifetime. E_B is considered as an intermediate state where the recombination and dissociation of charge carriers are triggered through this intermediate state. It is possible for the electron–hole pair to return to the initial state or be dissociated to the free charge carriers. This charge carrier dissociation is a competition between the separation rate, k_{diss}, and the recombination of charge carriers that is conducted through an intermediate phase or the CT state. In this model the probability of electron–hole pair dissociation, for a given electron–hole pair distance x, is given by

$$p(x,T,F) = \frac{k_{diss}(x,T,F)}{k_{diss}(x,T,F) + k_f(T)}, \tag{3}$$

depending on both temperature T and field strength F. The decay rate of the bound electron–hole pair to the ground state, k_f, is used as a fit parameter. Based on Onsager theory for field-dependent dissociation rate constants for weak electrolytes,[18,34] Braun derives the following expression for k_{diss}:

$$k_{diss}(x,T,F) = \frac{3R}{4\pi a^3}\exp(-E_B/K_BT)\,J_1(2\sqrt{-2b})/\sqrt{-2b}, \tag{4}$$

where $b = qF^3/(8\pi\varepsilon k_B^2T^2)$ and J_1 is the Bessel function of order 1. The decay rate of the bound electron–hole pair to the ground state, k_f, is used as a fit parameter (Eq. (3)). As polymer systems are subject to disorder, it is reasonable to assume that the electron–hole pair distance is not constant throughout the system.[18] As a result, it should be integrated over a distribution of separation distances

$$P(x,T,F) = \int_0^\infty p(x,T,F)f(a,x)\,dx, \tag{5}$$

$f(a,x)$ is a normalized distribution function given by the following equation[30]

$$f(a,x) = \frac{4}{\sqrt{\pi}a^3}x^2\exp(-x^2/a^2). \tag{6}$$

This leads to a modification of free charge carrier recombination terms by P, which describes the probability of the dissociation of a CT state, and consequently geminate recombination determined as,[18,31]

$$R_{\rm g} = R_{\rm lang}(1-P). \tag{7}$$

Another mechanism resulting in loss in organic solar cells is the indirect recombination by traps. To calculate the type of recombination, we take into account the trap assisted Shockley–Read–Hall (SRH) with the trap density $N_{\rm t}$ and the capture coefficient $C_{\rm t}$[37–39]

$$R_{\rm SRH} = C_{\rm t}N_{\rm t}\frac{np-n_i^2}{n+p+n_{\rm d}+p_0}, \tag{8}$$

which $n_{\rm d}$ and p_0 are characteristic charge carrier densities. For the sake of simplicity we assume a temperature-independent effective bandgap. The basic equations used in this simulation are the Poisson equation:

$$\frac{\rm d}{{\rm d}x}\psi(x) = \frac{q}{\varepsilon}(p(x)-n(x)), \tag{9}$$

where $\psi(x)$ is applied electric field and the current continuity equations:

$$\begin{aligned} J_n(x) &= \mu_n n(x)\psi(x) + D_n\frac{\rm d}{{\rm d}x}n(x),\\ J_p(x) &= \mu_p p(x)\psi(x) - D_p\frac{\rm d}{{\rm d}x}p(x). \end{aligned} \tag{10}$$

In these equations, J_n, J_p are electron current density, hole current density, and D_n and D_p are diffusion coefficients of electrons and holes, respectively. The charge concentration continuity equations for electrons and holes are:

$$\begin{aligned} \frac{\rm d}{{\rm d}t}n(x) &= \frac{1}{q}\frac{\rm d}{{\rm d}x}J_n(x) + G(x) - R(x),\\ \frac{\rm d}{{\rm d}t}p(x) &= \frac{1}{q}\frac{\rm d}{{\rm d}x}J_p(x) + G(x) - R(x), \end{aligned} \tag{11}$$

where G is the generation rate of free charge carrier result in the separation of exciton and R is recombination rate of charge carriers, meaning the total produced charge carriers are recombined inside the bulk and hence, we ignore the current gradient. In our study, we solve these equations via FDM by applying the boundary conditions and 100-nm active layer thickness. The scheme used to solve the Poisson and continuity equations is based on the work of Gummel.[40] In this scheme, first a guess is made for the potential and the carrier densities. With this guess, a correction $\delta\psi(x)$ to the guessed potential is calculated from the Poisson equation. This new potential is then used to update the carrier densities by solving the continuity equations.[40] Finally, by calculating the charge continuity equations, it is possible to calculate $J_{\rm sc}$, $V_{\rm oc}$, FF, cell efficiency and J–V characteristics in different doping concentrations. The calculation of the η, has been performed using the equation:

$$\eta = \frac{J_{\rm sc}V_{\rm oc}FF}{P_{\rm in}}, \tag{12}$$

where $P_{\rm in}$ is the incident light power.

3. Results and discussion

We have considered a typical BHJ OSC structure as shown in Fig. 1(a). In this paper, we assume that the absorbed photon directly generates a free electron–hole pair, and consequently, the charge drift-diffusion model has to be modified in order to suppress the electron–hole recombination into an exciton. The position 0 corresponds to the PEDOT/P3HT:PCBM interface and the position 100 to the P3HT:PCBM/cathode interface.

Table 1. The parameters that are used in numerical simulation.

Parameter	Symbol	Value	References
Active layer thickness/nm	x	100	[11], [13], [18], [30]
Temperature/K	T	300	–
Band gap/eV	$E_{\rm g}$	1.7	[18]
Electron mobility/cm^2/V·s	$\mu_{\rm e}$	2×10^{-5}	[14]
Hole mobility/cm^2/V·s	$\mu_{\rm h}$	2×10^{-4}	[14]
Dielectric constant/(F/cm)	$\varepsilon(\varepsilon_0)$	3.36×10^{-11}	[13]
Effective density of states/cm^{-3}	$N_{\rm c}$,$N_{\rm v}$	1.4×10^{18}	[30]
Incident sunlight power/W·m^{-2}	$P_{\rm in}$	1000	–

When an electron–hole pair is formed by absorbing light, there would be three possibilities for photogenerated electrons; i) First, they might accumulate at the cathode, ii) second, they could recombine with holes, and iii) third, they would move to the anode and accumulate. Electrons could recombine with the holes produced by light as well as with the holes coming from the anode with higher work function. In our simulation, different recombination models such as bimolecular or

Langevin recombination, SRH recombination or trap-assisted and geminate recombination, have been taken into account in numerical simulations. All parameters used in our numerical simulation are presented in Table 1.

Figure 2 shows J_{sc} with respect to p-dopant that J_{sc} improved by 12% by increasing the p-dopant from 10^{17} cm^{-3} to 5×10^{19} cm^{-3}.

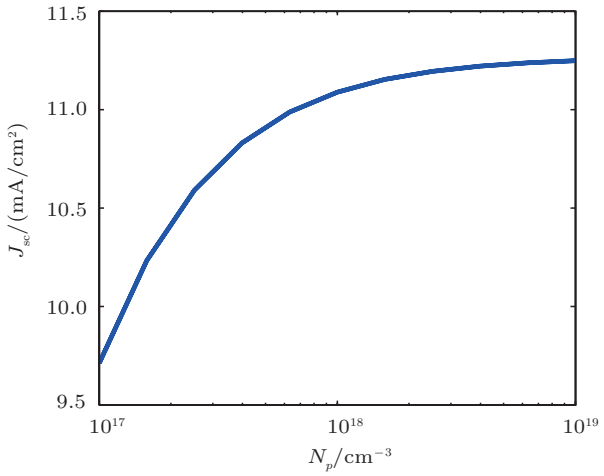


Fig. 2. (color online) J_{sc} as a function of p-dopant.

Simulation results for three n-dopant concentrations show that J_{sc} is not affected by three different n-dopant concentrations (n-type doping at 5×10^{17} cm^{-3}, 10^{18} cm^{-3}, and 5×10^{18} cm^{-3}). Results for different n-dopings are the same and in our simulation results, n-type doping variation did not affect the short circuit current. As it was shown, by increasing the p-dopant, J_{sc} reaches its maximum value (11.25 mA/cm^{-2}) at higher p-doping concentration ($>6\times10^{18}$ cm^{-3}). If doping is introduced, p-type dopants can partly compensate the space charge in the active layer, thus suppressing the recombination of free charges. Therefore, J_{sc} and the efficiency can be increased by doping.

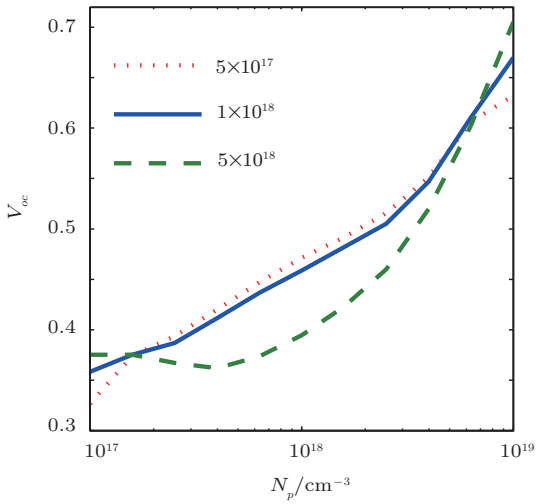


Fig. 3. (color online) V_{oc} as a function of p-dopant.

Figure 3 shows variation of V_{oc} as a function of p-dopant. As a result, V_{oc} increases twice (about from 0.35 V to 0.7 V) at p-doping and at $N_d=5\times10^{18}$ cm^{-3} n-dopant, V_{oc} increases by 10% in comparison with $N_d=5\times10^{17}$ cm^{-3}, but J_{sc} still has the same shape. If the recombination mechanism is bimolecular only (or Langevin type) the recombination rate under illumination and open circuit conditions equals the generation rate and is given by Eq. (1), but in this paper we calculate all recombination mechanisms which can occur in OSCs, thus our results have differences from previous published reports.[20,26] As it can be seen from Fig. 2 and Fig. 3, both J_{sc} and V_{oc} directly depend on active layer doping level, and this result concluded that dopants affected electron and hole concentration densities and Poisson's equation.

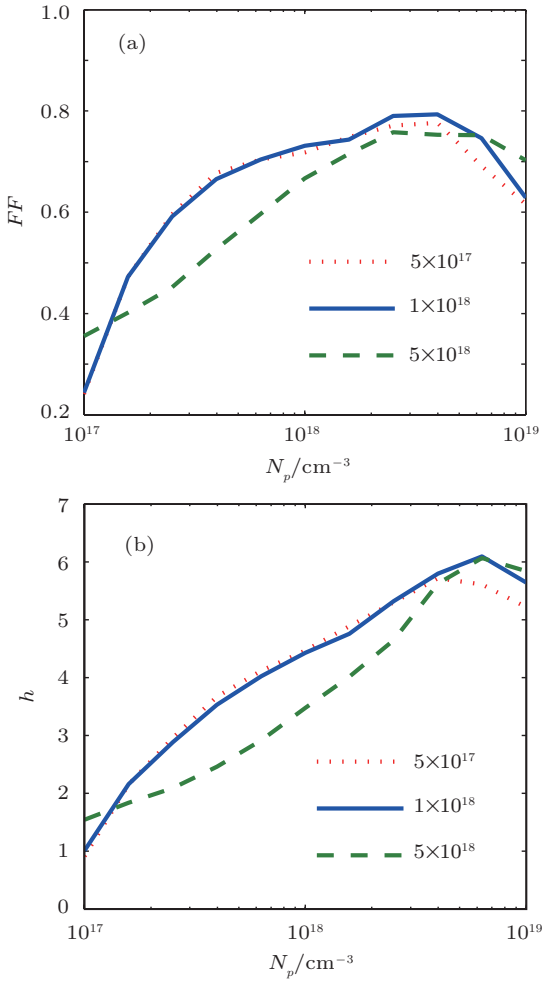


Fig. 4. (color online) (a) FF and (b) η as a function of p-dopant concentration, n-type doping are 5×10^{17} cm^{-3}, 10^{18} cm^{-3}, and 5×10^{18} cm^{-3}.

Figure 4(a) shows FF and figure 4(b) shows the η with respect to p-dopant in three n-dopant concentrations. FF increases by p-dopant concentration but in all three cases, it drops after it reaches a maximum point at about $N_p=4\times10^{18}$ cm^{-3}. FF in the case of $N_d=5\times10^{18}$ cm^{-3}, relatively lower in comparison with the other two n-dopants. In fact, FF falls down due to decreasing the ratio between charge generation and recombination rates in the active layer. On the other hand, this ratio increases from lower dopant to its peak at about $N_p=4\times10^{18}$ cm^{-3}. As it was shown in

Fig. 4(b), η reaches its maximum value, 6.2%, at somewhat higher doping ($N_p = 6 \times 10^{18}$ cm^{-3}) and after that, drops about 10%. As it was seen, optimum value for p-doping is about $N_p = 6 \times 10^{18}$ cm^{-3} and, according to the Figs. 4(a) and 4(b), the optimum value for n-dopant is $N_d = 10^{18}$ cm^{-3}, respectively. These results imply that doping considerably affects the performance of organic solar cells. To understand the decreasing in the observed trends in η we investigate the characteristic solar cell parameters. As it was seen from Figs. 2 and 3, at the high p-dopant, J_{sc} is constant and V_{oc} increases linearly, so in this case J_{max} and V_{max} or J–V curves determine η drops down.

For instance, in the case of the highest p and n-dopants, V_{oc} is higher in comparison with the optimum value (Fig. 3), but as it was shown in Fig. 5, the J–V characteristics curves have different forms. The J–V curves become flatter with increasing dopants, which means the FF decreases with increasing dopants, as confirmed in Fig. 4(a) and therefore, efficiency decreases.

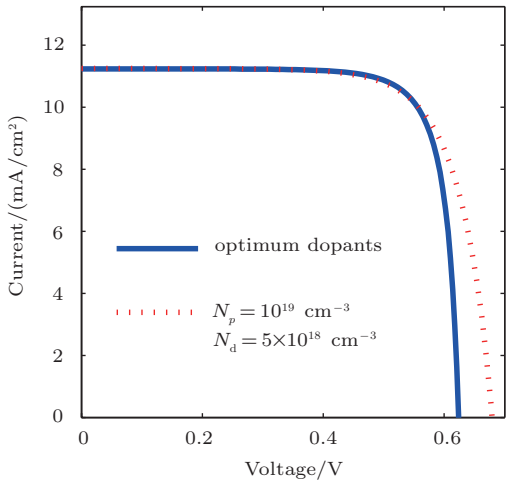


Fig. 5. (color online) The J–V characteristics for optimum and maximum dopants value.

4. Conclusion

We illustrate the influence of the doping level on the solar cell characteristics considering a P3HT:PCBM bulk heterojunction structure. We perform numerical simulation by drift-diffusion model where FEM has been taken into account in simulations. Results showed that by increasing the p-dopant from 10^{17} cm^{-3} to 10^{19} cm^{-3}, J_{sc} improved by 12% and V_{oc} increases linearly. The cell efficiency reaches its maximum value at somewhat higher doping ($N_p = 6 \times 10^{18}$ cm^{-3}) and after that, drops about 10%. We showed the optimum value for n- and p-doping concentrations derived from simulations, that the optimum value for the p-doping is about $N_p = 6 \times 10^{18}$ cm^{-3}, and for the n-dopant it is about $N_d = 10^{18}$ cm^{-3}. The J–V curves become flatter with increasing or decreasing dopants from optimum values, which means the FF decreases with increasing dopants, and therefore, the efficiency decreases. These results imply that the doping is very important since it enters through efficiency and it considerably affects the performance of organic solar cells.

References

[1] Brabec C J, Sariciftci N S and Hummelen J C 2001 *Adv. Funct. Mater.* **11** 15
[2] Krebs F C 2009 *Sol. Energy Mater. Sol. Cells* **93** 394
[3] Li G, Zhu R and Yang Y 2012 *Nat. Photon.* **6** 153
[4] Hoppe H and Sariciftci N S 2004 *J. Mater. Res.* **19** 1924
[5] Movla H 2016 *Optik* **127** 1814
[6] Wei M K, Lin C W, Yang C C, Kiang Y W, Lee J H and Lin H Y 2010 *Int. J. Mol. Sci.* **11** 1527
[7] Kappaun S, Slugovc C and List E J W 2008 *Int. J. Mol. Sci.* **9** 1527
[8] Liang C, Wang Y, Li D, Ji X, Zhang F and He Z 2014 *Sol. Energy Mater. Sol. Cells* **127** 67
[9] Tromholt T, Manceau M, Helgesen M, Carle J E and Krebs F C 2011 *Sol. Energy Mater. Sol. Cells* **95** 1308
[10] Zhou Y, Pei J, Dong Q, Sun X, Liu Y and Tian W 2009 *J. Phys. Chem. C* **113** 7882
[11] Movla H, Shahalizad A and Nezamabad A R 2014 *J. Opt. Quantum Electron.* **47** 621
[12] Rezzonico D, Perucco B, Knapp E, Roger Hausermann, Reinke N A, Muller F and Ruhstaller B 2011 *J. Photonics for Energy* **1** 011005
[13] Kotlarski J D, Blom P W M, Koster L J A, Lenes M and Sloof L H 2008 *J. Appl. Phys.* **103** 084502
[14] Fallahpour A H, Gagliardi A, Santoni F, Gentilini D, Zampetti A, Auf der Maur M and Di Carlo A 2014 *J. Appl. Phys.* **103** 184502
[15] Mahmoudloo A and Ahmadi-Kandjani S 2015 *Appl. Phys. A* **119** 1523
[16] Movla H, Rafi A M and Rafi N M 2015 *Optik* **126** 1429
[17] Movla H, Ghaffari S and Ahmadinasab H 2016 *Optik* **127** 1814
[18] Koster L J A, Smits E C P, Mihailetchi V D and Blom P W M 2005 *Phys. Rev. B* **72** 085205
[19] Nelson J, Kwiatkowski J J, Kirkpatrick J and Frost J M 2009 *Acc. Chem. Res.* **42** 1768
[20] Stelzl F F and Wurfel U 2012 *Phys. Rev. B* **86** 075315
[21] Ray B and Alam M A 2012 *Sol. Energy Mater. Sol. Cells* **99** 204
[22] Pfeiffer M, Leo K, Zhou X, Huang J S, Hofmann M, Werner A and Blochwitz-Nimoth J 2003 *Organic Electron.* **4** 89
[23] Gregg B A 2009 *J. Phys. Chem. C* **113** 5899
[24] Gregg B A 2009 *Soft Matter.* **5** 2985
[25] Shahalizad A, Ahmadi-Kandjani S, Movla H, Zakerhamidi M S, Omidi H, Massoumi B and Entezami A A 2014 *Opt. Mater.* **37** 760
[26] Trukhanov V A, Bruevich V V and Paraschuk D Y 2011 *Phys. Rev. B* **84** 205318
[27] Nollau A, Pfeiffer M, Fritz T and Leo K 2000 *J. Appl. Phys.* **87** 4340
[28] Veysel Tunc A, De Sio A, Riedel D, Deschler F, Da Como E, Parisi J and Von Hauff E 2012 *Org. Electron.* **13** 290
[29] Maennig B, Pfeiffer M, Nollau A, Zhou X, Leo K and Simon P 2001 *Phys. Rev. B* **64** 195208
[30] Mihailetchi V D, Koster L J A, Hummelen J C and Blom P W M 2004 *Phys. Rev. Lett.* **93** 216601
[31] Tress W, Leo K and Riede M 2012 *Phys. Rev. B* **85** 155201
[32] Halls J J M, Walsh C A, Greenham N C, Marseglia E A, Friend R H, Moratti S C and Holmes A B 2002 *Nature* **376** 498
[33] Onsager L 1938 *Phys. Rev.* **54** 554
[34] Braun C L 1984 *J. Chem. Phys.* **80** 4157
[35] Hausermann R, Knapp E, Moos M, Reinke N A, Flatz Th and Ruhstaller B 2009 *J. Appl. Phys.* **106** 10450
[36] Roichmann Y and Tessler N 2002 *Appl. Phys. Lett.* **80** 1948
[37] Shockley W and Read W T Jr 1952 *Phys. Rev.* **87** 835
[38] Sze S M 2005 *Physics of Semiconductor Devices*, 2nd edn. (New York: John Wiley Sons)
[39] Gorji N E, Movla H, Sohrabi F, Hosseinpour A, Rezaei M and Babaei H 2010 *Physica E* **42** 2353
[40] Gummel H K I 1964 *IEEE Trans. Electron. Dev.* **11** 455